Available online at www.sciencedirect.com
ScienceDirect
Journal of Energy Chemistry 22(2013)408–412
JOURNAL OF ENERGY CHEMISTRY
www.elsevier.com/locate/jngc

Coronal multi-walled silicon nanotubes

Yuanshuai Zhu[a†], Zhibei Qu[a,b†], Guilin Zhuang[a], Wulin Chen[a], Jianguo Wang[a*]

a. Institute of Industrial Catalysis, College of Chemical Engineering and Materials Science, Zhejiang University of Technology, Hangzhou 310032, Zhejiang, China; b. Department of Chemistry, East China Normal University, Shanghai 200241, China

[Manuscript received October 12, 2012; revised January 14, 2013]

Abstract

By means of first-principles density functional theory (DFT) calculations and molecular dynamics (MD) simulations, a series of coronal multi-walled silicon nanotubes (MWSiNTs) without or with hydrogen terminations are systematically identified. Notably, coronal MWSiNTs, where the interaction between the walls is preferable through covalent bonds rather than weak interaction, show better stability than CNT-like SiNTs. Moreover, they exhibit good elasticity with small Young's modulus. The investigation of the electronic structure demonstrates that they present metallic characteristics, which is in striking contrast to bulk silicon. Thus, the MWSiNTs may find important applications in electronic devices.

Key words

multi-walled silicon nanotubes (MWSiNTs); structural stability; electronic property; Young's modulus

1. Introduction

Since the discovery of carbon nanotubes (CNTs) in 1991, extensive research has revealed that the unique structural and electronic properties of tubular materials are distinctly different from those of their bulk [1]. Silicon is an important atom belonging to the same group (group IV) as carbon in the periodic table. However, Si has more electrons than C, resulting in higher polarizability and stronger dispersion force [2]. Nanotubes composed of Si atoms [3,4] have attracted considerable attention partly because of their apparent compatibility with Si-based microelectronics, and they are thus very promising in various applications of magnetics [5], photoelectronics [6], electrodes [7], transistors and field emission devices [8]. Particularly, Si nanotubes (SiNTs) have been regarded as the promising candidates for gas storage. SiNTs demonstrated considerably higher adsorption capacity of H_2 than the isomer CNTs [9]. In addition, Balilehvand et al. [10] performed a combination of *ab initio* quantum mechanical (QM) calculations and canonical Monte Carlo (CMC) simulations to investigate the effects of size, temperature, and pressure on the adsorption and separation behavior of H_2 and CH_4. They found the remarkable enhancement of both H_2 and CH_4 adsorption capacity on the SiNTs compared to the CNTs due to stronger van der Waals (VDW) attractions.

However, unlike CNTs, the successful synthesis of analogous SiNTs based on rolled-up graphene-like sheets is rather difficult, which may obstruct further study of their physical and chemical properties. This is mainly attributed to the rather weak π-bonds [3] as well as the flexible coordination geometry of silicon atoms, such as five- and six-coordinate [11−13]. Sha et al. [14] reported that the multiwalled SiNTs (MWSiNTs) can be efficiently synthesized within nano-channels of an alumina substrate by chemical vapor deposition. Tang et al. [15] prepared self-assembled SiNTs from silicon monoxide under supercritically hydrothermal conditions. Note that only MWSiNTs, where the interaction between the walls prefers covalent bonds [15], rather than single-walled SiNTs (SWSiNTs) can only be experimentally obtained under appropriate conditions. Theoretically, Fagan et al. [16] examined the electronic and structural properties of SiNTs and CNTs by density functional theory (DFT) and found that they are similar to each other. Zhang et al. [17] showed that SiNTs adopted corrugated tubular structures via semiempirical calculations. Moreover, Zeng et al. [18,19] demonstrated the possible existence of square, pentagonal and hexagonal SWSiNTs (Figure 1) and they suggested that those SiNTs are metals rather than semiconductors with wide-gap. However, to the best of our knowledge, in-depth theoretical investigations on MWSiNTs [4,20] are very rare. In this work, we employed first-principles DFT calculations and molecular dynamics (MD) simulations to explore four kinds of hypothetical coronal MWSiNTs with emphasis on their geometric, electronic and elastic properties.

* Corresponding author. † These authors contributed equally to this work; Tel: +86-571-88871037; Fax: +86-571-88871037; E-mail: jgw@zjut.edu.cn
This work was supported by the National Natural Science Foundation of China (No.20906081, 21176221, 21101137 and 21136001), Zhejiang Provincial Natural Science Foundation of China (No. R4110345) and the Program for New Century Excellent Talents in University (NCET-10-0979).

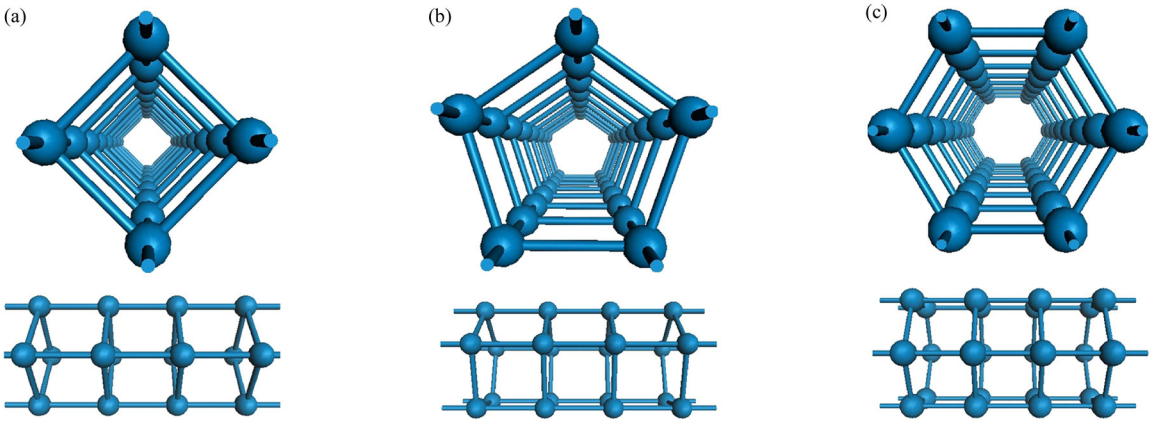

Figure 1. Schematic models of single-walled silicon nanotubes. (a) Square, (b) pentagonal, (c) hexagonal

2. Computational details

The first-principles DFT calculations were performed using the DMol^3 package [21,22]. The exchange-correlation interaction was treated within the generalized gradient approximation (GGA) in the form of Perdew, Burke and Ernzerhof (PBE) [23]. All the electron treatment and double numerical basis set plus polarization functions (DNP) were utilized [21,22]. The convergence threshold in energy and force was set at 1×10^{-5} eV and 5×10^{-2} eV/Å, respectively. The Brillouin zone integrations were carried out by a $1\times1\times6$ k-mesh according to Monkhorst-Pack scheme [24]. The MWSiNTs were placed in supercells with spacings of at least 15 Å to avoid drawbacks in terms of interaction between the tubes. Typically, the binding energy (E_b) was calculated as:

$$E_b = (nE_{Si} - E_{NT})/n \quad (1)$$

where, n is the number of Si atoms; E_{Si} and E_{NT} are the energies of silicon atom and MWSiNTs, respectively.

MD simulations were carried out with the GULP code [25] under constant volume and constant temperature conditions (NVT). Tersoff forcefield [26], which is verified to yield nearly the same melting point (1684 K) as the measurement (1683 K) for bulk Si, was employed. The 20-unitcell nonperiodic superstructures from optimized previous structures by DMol^3 package were equilibrated at various temperatures from 298 K to 1200 K. At each site, the simulation in NVT ensemble was lasted for 500 ps with a time step of 1.0 fs, while the temperature was controlled by Nosé thermostat [27].

3. Results and discussion

Inspired by the distinct structures of MWSiNTs and SWSiNTs [18,28,29], we attempt to build up four types of MWSiNTs on the basis of Euclidean geometry. In two of these cases, a central *n*-ring is surrounded by a belt of *n* equivalent fused rings of size *m*, which is labeled as (*m*, *n*). To satisfy a plane, only two possible solutions are obtained, including (6, 6) and (5, 10). Both of patterns, as depicted in Figure 2(a) and 2(b), can be viewed as integrations of hexagonal, pentagonal SWSiNTs with fused sides. Two more analogues are built up from square, pentagonal and hexagonal SWSiNTs, binding with each other, as shown in Figure 2(c) and 2(d). Scrutinizing the structures of coronal MWSiNTs can find that 2D polygon-silicon layers bridge with vertical Si–Si bonds and lead to a 3D multi-walled tube. It should be noted that five-coordinate silicon atoms exist in these four coronal MWSiNTs. Although the previous work witnessed that hyper-coordinate silicon can energetically exist in elementary substance [12] and some chelates [13], five-coordinate silicon atoms are seldom found in periodic nanostructures. The optimized geometries reveal that four coronal MWSiNTs maintain their regular polygons with amazingly pretty symmetry of C_6, C_{10}, C_6 and C_{10}. The internal diameters of the hexagon, decagon, dodecagon and icosagon MWSiNTs are 4.93 Å, 8.10 Å, 9.86 Å and 16.42 Å, respectively. The average angles of the polygons approximate to 120°, 108° and 90° for hexagon, pentagon and square, respectively. The average bond length of Si–Si (2.52 Å) in the layer is larger than that of Si–Si single bond (2.38 Å as calculated), while the vertical Si–Si bond distance between the layers is about 2.64 Å.

To explore the electronic properties, we computed the band structure (BS) of coronal MWSiNTs. It was found that they all show similar electronic structures. Therefore, only the band structure of decagonal coronal MWSiNT is presented in Figure 2(e) and discussed. It can be seen that the whole energy bands cross the Fermi level from conduction band to valence band are widely dispersed in the vicinity of Fermi level, revealing that decagonal coronal MWSiNT exhibits metallic behavior. Compared with that of pentagonal SWSiNT previously reported, the metallicity of decagonal coronal MWSiNTs is more obvious, owing to the mixed state of hypercoordinated silicon atoms. Therefore, the obtained results by DFT calculations uncover that the hyper-coordinated silicon atoms play an important role in the electronic structures of these coronal MWSiNTs. Herein, it is mentioned that the characteristics of coronal MWSiNTs are remarkably different from those of bulk Si (a narrow band gap of 0.90 eV), CNT-

like silicon nanostructures (a narrow band gap depending on structural details) and DWSiNTs with faceted wall surface (a wide band gap of 2.18 eV). Scrutinizing their structures reveals that the decrease of band gap may be related to the fact that regular geometry of MWSiNTs facilitates 3*p* orbits of silicon effective overlap so as to let 3*p* band disperse around the Fermi level. The phenomenon is in good agreement with the previous report [30].

To further investigate the effect of hyper-coordinated silicon on electronic properties, calculations on the hydrogen-terminated MWSiNTs (Figure 3) are employed since the surface termination of nanotubes, such as hydrogen-termination or oxygen-termination, usually has significant effect on electronic band structure [20]. However, H-terminated coronal MWSiNTs, where all the silicon atoms are five-coordinated, behave similar electronic properties with the pristine ones.

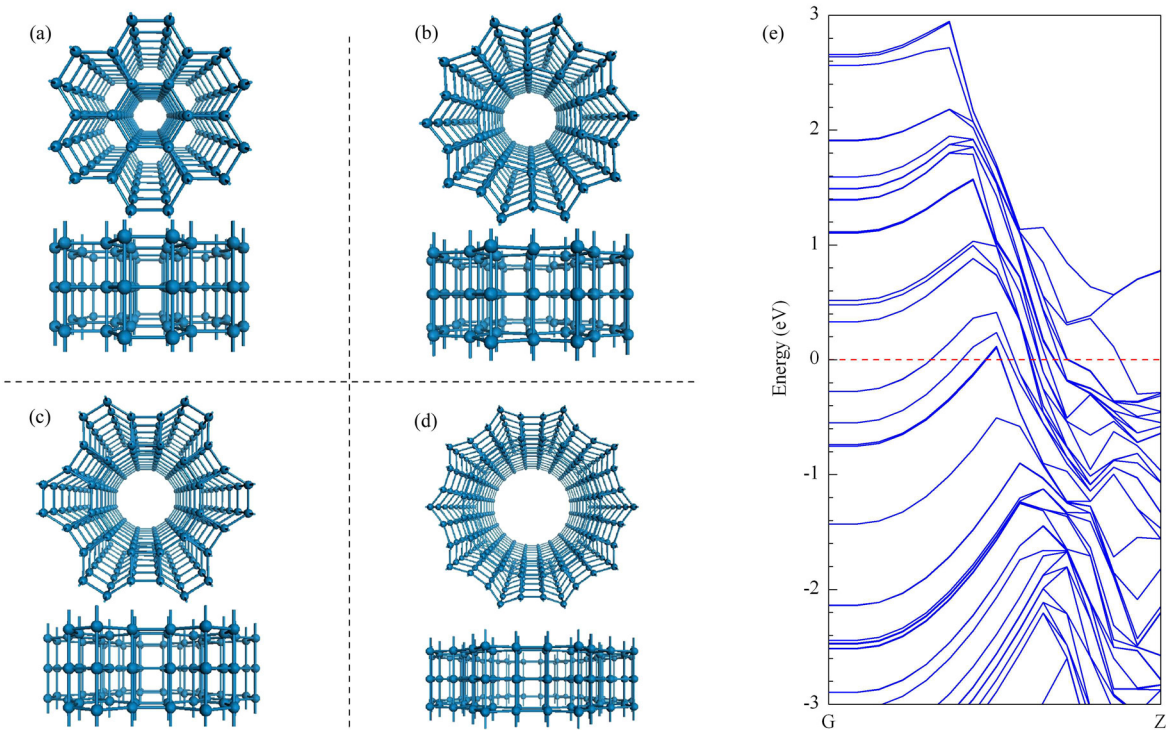

Figure 2. Perspective projecting geometries of side and top views of optimized structures of coronal MWSiNTs with hexagon (a), decagon (b), dodecagon (c) and icosagon (d) for the internal wall, respectively; (e) band structure for decagonal coronal MWSiNTs (the Fermi energy is set to zero)

Are the hypothetical coronal MWSiNTs stable? In order to answer the question, four evidences are given from different aspects. First, coronal MWSiNTs are local stable configurations derived from optimizations by DMol^3 code with DNP basis set, as well as CASTEP program [31] with an ultrasoft pseudopotential method [32]. Second, the binding energy of coronal MWSiNTs is relatively large (5.72 eV/atom), which may show strong covalent bonds in the nanotubes. The binding energy of coronal MWSiNTs (1.54 eV/atom) is larger than that of (5, 5) CNTs-like SiNTs (4.18 eV/atom), suggesting that coronal MWSiNTs are much more energetic than (5, 5) CNTs-like SiNTs thermodynamically. Third, the prototype moieties of our coronal MWSiNTs, namely, SWSiNTs, are believed to be stable by previous researchers using classical MD simulations [19,29]. However, the binding energy of our coronal MWSiNTs (5.72 eV/atom) is larger than that of the most stable SWSiNT (5.59 eV/atom). Finally, the kinetic stability of coronal MWSiNTs is very good, as indicated by the results of MD simulations. A 20-layer non-periodic superstructure is applied in the calculation. Below 900 K, all the four nanotubes preserve their geometries very well, while above 1000 K the coronal MWSiNTs transform to amorphous silicon nanowire. Accordingly, once formed, coronal MWSiNTs can well maintain their structural integrity at least up to 900 K, as shown in Figure 4.

The Young's modulus of 3D bulk is known as a second partial derivative, as presented:

$$Y = \frac{1}{V_0}\left(\frac{\partial^2 E_\mathrm{b}}{\partial \varepsilon^2}\right)_{\varepsilon=0} \tag{2}$$

where, V_0 is the equilibrium volume; E_b is the binding energy of the nanotube; and ε stands for the strain. However, the Young's modulus of MWSiNTs is difficult to be obtained owing to the ambiguous cross-sectional area of the tube, which obstructs the clarification of V_0. Thus, the alternative Young's modulus (Y_c) specialized for MWNTs was performed based on the modified Hernánde's method [33], as defined:

$$Y_c = \frac{1}{c_0}\left(\frac{\partial^2 E_b}{\partial \varepsilon^2}\right)_{\varepsilon=0} \quad (3)$$

where, c_0 is the unit-cell length of the supercell. Given that $V_0 = c_0 S_c$, one can resume the usual definition by simply dividing by S_c: $Y = Y_c/S_c$, where S_c stands for the cross-sectional area of coronal MWSiNT, if a particular consuetude is adopted. Then we compare Y_c values of the MWSiNTs and CNTs, which have similar diameters for each internal wall (Figure 5). The (6, 6), (10, 10), (10, 0) and (20, 0) CNTs are employed in this work, and the calculated data is in good consistency with previous work. It can be obviously seen that Y_c of coronal MWSiNTs and CNTs goes up with the diameter increase. However, MWSiNTs exhibit much smaller Young's modulus. Thus, coronal MWSiNTs are more flexible than CNTs, implying MWSiNTs feature better elastic properties. It may be attributed to the relatively weak vertical Si–Si bond along the tube. It is noteworthy that the Young's modulus of coronal MWSiNTs is at the same order of magnitude as those of BNNTs and SiCNTs (all arranging from 0.3 to 0.7 TPa·nm^2) [34].

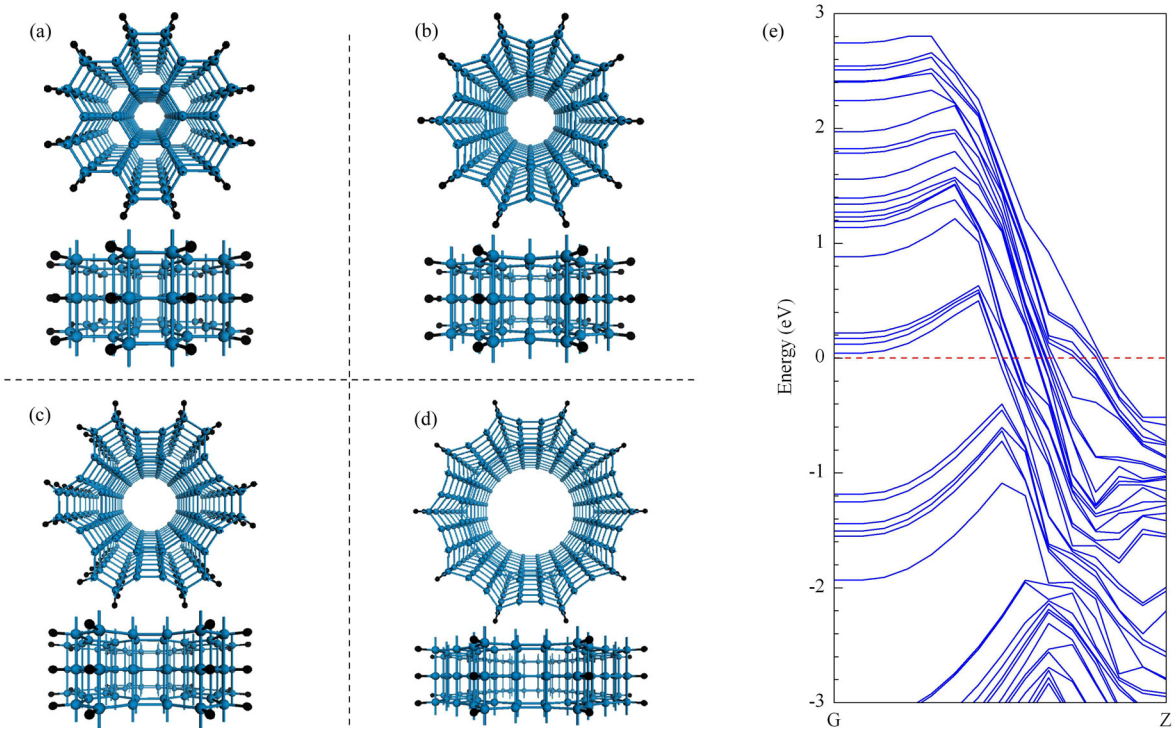

Figure 3. Perspective projecting geometries of side and top views of hydrogen-terminated coronal MWSiNTs with hexagon (a), decagon (b), dodecagon (c) and icosagon (d) for the internal wall, respectively; (e) band structure for H-terminated decagonal coronal MWSiNT (the Fermi energy is set to zero)

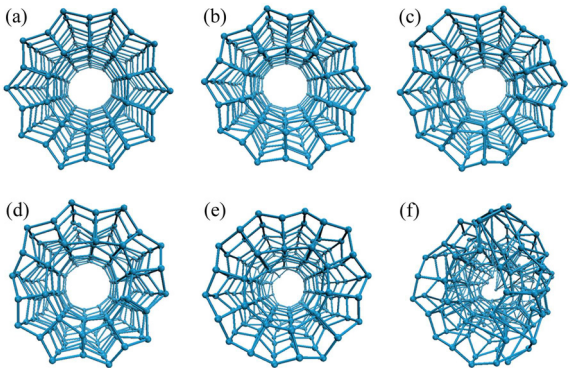

Figure 4. The structures at (a) 300, (b) 500, (c) 700, (d) 900, (e) 1000 and (f) 1200 K under NVT ensemble MD simulations

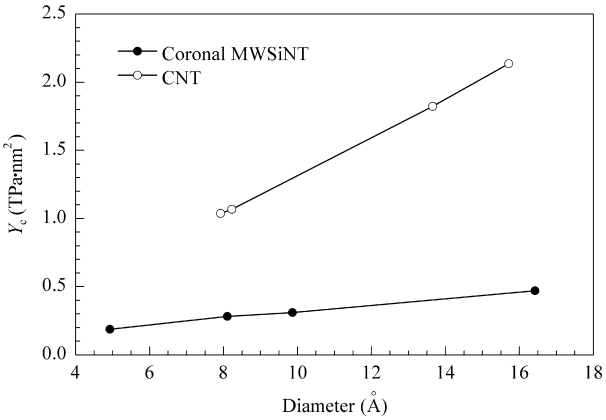

Figure 5. Young's modulus (Y_c) of coronal MWSiNTs and different CNTs

4. Conclusions

In summary, by DFT calculations and MD simulations we build up four novel coronal MWSiNTs with a large ratio of five-coordinated silicon atoms. It is found that the coronal MWSiNTs exhibit stable and high symmetric geometries as well as rather good elastic properties with small Young's modulus. The coronal MWSiNTs present metallic characteristics, which is in striking contrast to bulk silicon and CNT-like SiNTs. It is mentioned that our result is in good agreement with that reported by Ni et al. [6]. On one hand, our study may pay an effective way to explain the structures of MWSiNTs and thereby suggesting the possibility of synthesizing coronal MWSiNTs. On the other hand, the special feature of coronal MWSiNTs, derived from the prototype structures of SWSiNTs, may make them more attractive in these fields of electronic nanodevices.

References

[1] Iijima S. *Nature*, 1991, 354(6348): 56
[2] Teo B K, Sun X H. *Chem Rev*, 2007, 107(5), 1454
[3] Perepichka D F, Rosei F. *Small*, 2006, 2(1): 22
[4] Guo L J, Zheng X H, Zeng Z. *Phys Lett A*, 2011, 375(47): 4209
[5] Singh A K, Briere T M, Kumar V, Kawazoe Y. *Phys Rev Lett*, 2003, 91(14): 146802
[6] Ni M, Luo G F, Lu J, Lai L, Wang L, Jing M W, Song W, Gao Z X, Li G P, Mei W N, Yu D P. *Nanotechnology*, 2007, 18(50): 505707
[7] Song T, Xia J L, Lee J H, Lee D H, Kwon M S, Choi J M, Wu J, Doo S K, Chang H, Il Park W, Zang D S, Kim H, Huang Y G, Hwang K C, Rogers J A, Paik U. *Nano Lett*, 2010, 10(5): 1710
[8] Pei L Z, Wang S B, Fan C G. *Recent Pat Nanotechnol*, 2010, 4(1): 10
[9] Lan J H, Cheng D J, Cao D P, Wang W C. *J Phys Chem C*, 2008, 112(14): 5598
[10] Balilehvand S, Hashemianzadeh S M, Razavi S, Karimi H. *Adsorpt-J Int Adsorpt Soc*, 2012, 18(1): 13
[11] Nigam S, Majumder C, Kulshreshtha S K. *J Chem Phys*, 2006, 125(7): 074303
[12] Chang K J, Cohen M L. *Phys Rev B*, 1985, 31(12): 7819
[13] Kost D, Kalikhman I. *Acc Chem Res*, 2009, 42(2): 303
[14] Sha J, Niu J J, Ma X Y, Xu J, Zhang X B, Yang Q, Yang D. *Adv Mater*, 2002, 14(17): 1219
[15] Tang Y H, Pei L Z, Chen Y W, Guo C. *Phys Rev Lett*, 2005, 95(11): 116102
[16] Fagan S B, Baierle R J, Mota R, da Silva A J R, Fazzio A. *Phys Rev B*, 2000, 61(15): 9994
[17] Zhang R Q, Lee S T, Law C K, Li W K, Teo B K. *Chem Phys Lett*, 2002, 364(3-4): 251
[18] Bai J, Zeng X C, Tanaka H, Zeng J Y. *Proc Natl Acad Sci U S A*, 2004, 101(9): 2664
[19] Yan B H, Zhou G, Zeng X C, Wu J, Gu B L, Duan W H. *Appl Phys Lett*, 2007, 91(10): 103107
[20] Zhao M W, Zhang R Q, Xia Y Y, Song C, Lee S T. *J Phys Chem C*, 2007, 111(3): 1234
[21] Delley B. *J Chem Phys*, 1990, 92(1): 508
[22] Delley B. *J Chem Phys*, 2000, 113(18): 7756
[23] Perdew J P, Burke K, Ernzerhof M. *Phys Rev Lett*, 1996, 77(18): 3865
[24] Monkhorst H J, Pack J D. *Phys Rev B*, 1976, 13(12): 5188
[25] Gale J D, Rohl A L. *Mol Simulat*, 2003, 29(5): 291
[26] Tersoff J. *Phys Rev Lett*, 1986, 56(6): 632
[27] Nosé S. *J Chem Phys*, 1984, 81(1): 511
[28] Wang X W, Huang Z, Wang T, Tang Y W, Zeng X C. *Physica B*, 2008, 403(12): 2021
[29] Lee R K F, Cox B J, Hill J M. *Nanoscale*, 2010, 2(6): 859
[30] Zhang R Q, Hou C, Gao N, Wen Z, Jiang Q. *ChemPhysChem*, 2011, 12(7): 1302
[31] Segall M D, Lindan P J D, Probert M J, Pickard C J, Hasnip P J, Clark S J, Payne M C. *J Phys-Condens Mater*, 2002, 14(11): 2717
[32] Vanderbilt D. *Phys Rev B*, 1990, 41(11): 7892
[33] Hernández E, Goze C, Bernier P, Rubio A. *Phys Rev Lett*, 1998, 80(20): 4502
[34] Li Y F, Li F Y, Zhou Z, Chen Z F. *J Am Chem Soc*, 2011, 133(4): 900